ELSEVIER

Journal of Nuclear Materials 297 (2001) 251–261

journal of nuclear materials

www.elsevier.com/locate/jnucmat

Irradiation effects on toughness behaviour and microstructure of VVER-type pressure vessel steels

J. Böhmert *, H.-W. Viehrig, A. Ulbricht

Forschungszentrum Rossendorf, Institut für Sicherheitsforschung, Abt. Material- u. Komponentensicherheit, P.O. Box 510 119, D-01314 Dresden, Germany

Received 19 March 2001; accepted 29 May 2001

Abstract

The irradiation sensitivity and the annealing behaviour were studied on seven different heats from VVER 440 and VVER 1000-type reactor pressure vessel steels. The specimens were irradiated at the Rheinsberg prototype VVER 2 reactor to mean neutron fluences between 43 and 127.6×10^{18} n/cm^2 [$E > 0.5$ MeV]. Toughness and strength properties were determined and the microstructure was analysed using the small angle neutron scattering (SANS) technique. There is an obvious correlation between the irradiation-induced changes of transition temperature, hardness and volume fraction of microstructural features of radii up to 2 nm. The main parameters of influence are the neutron fluence and the nickel content. The nickel-containing VVER 1000-type pressure vessel steel is more sensitive to irradiation than the VVER 440-type steel which has a low nickel content. For the latter, the sensitivity to radiation embrittlement depends on the copper and phosphorus contents. Annealing at 475°C (100 h) reduces the irradiation effect but not completely in every case.

1. Introduction

The results from the first surveillance tests for the VVER 440-type reactor Loviisa 1 [1] showed a higher shift of the transition temperature than expected and created doubts about the correctness of the Russian approach of the irradiation embrittlement assessment. In consequence, an extensive irradiation programme at the PWR VVER 2 of the Rheinsberg nuclear power plant was initiated. The programme should enhance the database for irradiated VVER pressure vessel steels. Therefore a broad variety of RPV steels, covering both the typical manufacturer's specifications of the different VVER models and test heats with modified composition or manufacturing, were selected and irradiated under conditions that are comparable with the VVER. In particular the programme was established to diagnose the irradiation embrittlement sensitivity, to assess the Russian code approach and the irradiation embrittlement trend curves, to determine fracture mechanics parameters and to characterize the annealing behaviour.

The post-irradiation mechanical tests have been performed by several German laboratories within the framework of a German–Russian cooperation project. The Forschungszentrum Rossendorf (FZR) has been involved in this work. The results of the mechanical testing have already been published [2,3].

In addition to the original working programme small angle neutron scattering (SANS) experiments have been addressed to study the interrelation between the effects of the irradiation on the mechanical behaviour and the microstructural evolution. This investigation is expected to provide a fuller understanding from the physical point of view.

The comparison of the results of mechanical tests and SANS experiments is presented in this paper.

* Corresponding author. Tel.: +49-351 260 3186; fax: +49-351 260 2205.

E-mail address: j.boehmert@fz-rossendorf.de (J. Böhmert).

0022-3115/01/$ - see front matter
PII: S0022-3115(01)00636-5

2. Irradiation programme

2.1. Materials investigated

The materials tested were

- 4 heats from 15Kh2MFA (15CrMoV2) VVER 440-type base metal designated by code R1, R2, R3, and D25,
- 2 heats from 15Kh2NMFAA (15CrNiMoV2) VVER 1000-type base metal designated by code R16, and R17,
- 1 heat from 10KhGNMAA (10CrMnNiMo) VVER 1000-type weld metal designated by code R19.

The chemical composition is given in Table 1. The heats R2, R3, and D25 meet the chemical composition required for the active core shells of the VVER 440/230-type [4] and are characteristic for the RPVs from the Russian production line of the 1970s. R1 has a too low content of chromium. R16, R17, and R19 are representative for the first VVER 1000/320 units although the content of phosphorus is a little too high related to the specification [4]. The dominant microstructure consists of granular bainite, only the 15Kh2MFA heats contain a low content of pro-eutectoid ferrite. There are clear differences in the prior austenite grain size ranging from a mean intercept length of 45 μm for R16 to 110 μm for R2 and R17. The content of non-metallic inclusions was low in every case.

From each heat, Charpy V-notch standard and pre-cracked specimens were machined according to the Russian standards. The specimens were taken from the 1/4 to 3/4 thickness position and orientated in L–S, T–S, and L–T orientation (nomenclature according to ASTM E 399).

2.2. Irradiation conditions

The specimens were irradiated in the core-near high flux channels of the Rheinsberg VVER 2 reactor during one operation cycle. The VVER 2 is a PWR prototype with 70 MW electric power and an inlet temperature of cooling water of 245°C. It is especially suitable as irradiation facility because the large cross-section of the high-flux channels allows to irradiate large and numerous specimens. However, the large cross-section causes a high radial gradient of neutron flux. In consequence of this, the fluences of different specimens of one set could vary up to a factor of 2. The results of the tests were, therefore, corrected to the same mean fluences. The base for this procedure was detailed neutron dosimetry including the gamma-spectrometric analysis of activation detectors and an extensive three-dimensional Monte-Carlo transport calculation of the neutron field. The details of the irradiation, the neutron fluence determination and the correction procedure are presented by Barz et al. [5] and Viehrig et al. [6]. The mean fluences reached during the irradiation are given with the testing results. Mean neutron fluxes amounted to $1–4 \times 10^{12}$ n/cm^2 s [$E > 1$ MeV] which is comparable with the flux at the surveillance position of a VVER 440 with full core loading. The mean irradiation temperature was estimated to 255°C.

To ensure intense cooling, the specimens were placed in open irradiation rigs with direct contact to the coolant. A thin nickel layer on the surface of specimens should prevent corrosion attacks. Unfortunately, during the long storage period after irradiation the layer was partly destroyed and the surface was corroded. In these cases the specimens were touched up [2,3].

3. Post-irradiation testing procedures

3.1. Mechanical tests

The specimens were tested by Charpy V impact tests, fracture toughness measurements according to ASTM E 1921–97, and hardness tests.

The Charpy impact tests were performed using an instrumented 300 J impact-pendulum with a DIN tup in the temperature range of −150°C to +300°C and evaluated according to ISO/DIN 14556. Geometry, lateral extension and fibrous fracture fractions were measured by a video measuring system. Each individual Charpy

Table 1
Chemical composition of the steels investigated, percentage by mass (Fe balance)

Type	Code	C	Si	Mn	Cr	Ni	Mo	V	S	P	Cu
15Kh2MFA	R 1	0.14	0.24	0.45	2.13	0.27	0.61	0.25	0.011	0.011	0.10
	R 2	0.14	0.25	0.44	2.82	0.12	0.68	0.29	n.m.[a]	0.014	0.12
	R 3	0.17	0.26	0.45	2.60	0.12	0.67	0.30	n.m.	0.024	0.12
	D 25	0.16	0.22	0.49	2.74	0.10	0.68	0.32	n.m.	0.017	0.11
15Kh2NMFAA	R 16	0.14	0.31	0.48	2.21	1.11	0.57	0.10	n.m.	0.012	0.07
	R 17	0.15	0.27	0.47	2.08	1.30	0.57	0.10	n.m.	0.013	0.13
10KhGNMAA	R 19	0.09	0.38	1.14	1.66	1.71	0.63	0.01	0.010	0.012	0.04

[a] n.m. – Not measured.

data set was fitted to a hyperbolic tangent function. Transition temperature and upper shelf energy are related to the fit function.

Testing of the pre-cracked specimens is based on the master curve concept according to ASTM E 1921–97 and is not described in this paper. The reader is referred to Viehrig et al. [2]. The hardness was determined by Vickers hardness tester with a load of 10 kp (98.1 N). The tests were performed by making 10 measurements for each sample made from Charpy specimens.

Specimens from all heats were tested in the unirradiated (U) and the irradiated (I) state. Furthermore, specimens were annealed 100 h at 475°C in argon atmosphere and also tested (post-irradiation annealed state – IA).

3.2. Small angle neutron scattering (SANS)

SANS experiments were carried out at the BENSC V4 spectrometer of HMI Berlin (Germany) [7], at the D11 spectrometer of ILL Grenoble (France) [8] and the PAXE spectrometer of LLB CEA Saclay (France) [9], using 10 mm × 10 mm × 1 mm discs cut from tested Charpy specimens. For the different instruments nearly the same experimental conditions were selected. A wavelength of 0.5 or 0.6 nm with total width at half maximum of wavelength of 10% of the nominal wavelength was used. The data were measured at mainly two different sample–detector distances of 1.1 and 5 m, resulting in a scattering vector interval of about 0.1–3.0 nm^{-1}. The neutron beam incident on the sample was 7 mm in diameter. The scattering intensity was measured with a two-dimensional position-sensitive detector. During the measurement a saturating magnetic field of 1.4 T was applied perpendicular to the incident neutron beam.

The calibration was performed using a water standard or the direct beam method. Additionally, the same sample was measured at different instruments. In this case, there were no significant differences. The data [10] were processed by software routines of BENSC, ILL and LLB to determine the nuclear and magnetic macroscopic scattering cross-section versus the scattering vector. Under the assumption that the scattering structural defects are non-ferromagnetic, the volume fraction and the size distribution of the scatterers can be estimated. For the latter the indirect Fourier transformation method according to Glatter [11] was used. The evaluation procedure is presented in more detail in [12,13].

4. Results

4.1. Mechanical testing

The data derived from the Charpy impact tests for all the heats tested are represented in Table 2. Apart from the two heats R1 and R2 of VVER 440-type base metal all investigated materials exhibit a high toughness in the unirradiated state. Particularly, the Charpy toughness parameters of the VVER 1000 base metal (15Kh2NMFAA) are excellent. As usual the toughness of the weld metal is lower but sufficient to the Russian specification. The 15Kh2MFA heats R1 and R2 are at the boundary of the guaranteed mechanical transition temperature TT_o. As the procedure of Charpy testing did not meet the Russian regulation for the determination of TT_o, this question cannot be decided definitely.

Irradiation within the investigated fluence range from 23.2 to $138 \times 10^{18}/cm^2$ [$E > 0.5$ MeV] causes a clear degradation of the toughness. Irradiation shifts the ductile-to-brittle transition temperature TT to higher temperatures, lowers the upper shelf energy USE and often changes the shape of the Charpy energy–temperature curve. Figs. 1 and 2 illustrate these phenomena for a heat of 15Kh2MFA (R3) and the VVER 1000 weld metal (R19). The figures also show the low effect of fluence gradient within the specimen set. The fluence correction (I_{corr}) according to the procedure in [6] does not significantly change the course of the energy–temperature curve. This is characteristic for the other results as well.

The Russian standard PNAE G-7-002-86 (quoted in [14]) evaluates the effect of irradiation with the analytical expression

$$\Delta TT = A_F \sqrt[3]{\Phi}, \tag{1}$$

where $\Delta TT = TT_o - TT_{irr}$ is the shift of the transition temperature TT due to irradiation, A_F is the irradiation embrittlement coefficient and Φ the neutron fluence, in 10^{18} n/cm^2, $E > 0.5$ MeV.

The irradiation embrittlement coefficient A_F can be estimated from data measured. The results are also summarized in Table 2. The values range from 7.4 for the 15Kh2MFA heat R2 to 47.5 for the weld metal R19. This means that for typical end of life fluences $>10^{20}$ n/cm^2 [15] the transition temperature shifts would be between 20°C and >220°C. Whereas a shift of 20°C proves an excellent irradiation resistance, a shift of more than 220°C is not acceptable even if the transition temperature is low in the initial state.

The mean values of the hardness measurements are given in Table 3. In the unirradiated initial state there are clear differences in hardness (and strength as well) of the different heats, comparable with the differences in the transition temperature. In principle, the transition temperature correlates to the hardness (or to the yield strength) for each type of steel as showed in Fig. 3. Irradiation increases the hardness in every case. A hardness-related irradiation hardening coefficient A_F^{HV} formally defined correspondingly to Eq. (1) from the

Table 2
Results of the Charpy V tests of unirradiated (U), irradiated (I) and post-irradiation annealed (IA) specimens

Type	Code	State	Φ_{mean} (10^{18}/cm^2)[a]	TT_{48} (°C)[b,c]	ΔTT_{48} (K)[b,c]	R^{TT}[d]	USE (J)[e]	ΔUSE (J)	R^{USE}[f]	A_F[g]
15Kh2MFA	R1	U		0			199			
		I	43.6	31	31		164	−35		8.8
		IA		11	11	0.65	171	−28	0.2	
	R2	U		−55			211			
		I	80.7	−23	32		178	−33		7.4
		IA		−57	−2	1.07	227	16	1.48	
	R3	U		7			171			
		I	45.7	54	47		110	−61		13.1
		IA		14	7	0.85	138	−33	0.46	
	D25	U		−70			160			
		I	127.6	6	76		100	−60		15.1
		IA		−44	26	0.66	137	−23	0.62	
15Kh2NMFAA	R16	U		−81			196			
		I	46	−16	65		125	−71		18.1
		IA		−39	42	0.35	188	−8	0.89	
	R17	U		−48			196			
		I	72.7	76	124		149	−47		29.7
		IA		−46	−3	0.98	202	6	1.12	
10KhGNMAA	R19	U		−16			110			
		I	65.1	175	191		60	−50		47.5
		IA		−1	15	0.92	120	10	1.2	

[a] Φ_{mean} – Mean fluence [$E > 0.5$ MeV] (corresponding to approx. 10^{-3} dpa).
[b,c] TT_{48}, ΔTT_{48} – Transition temperature and shift of TT related to 48 J.
[d] R^{TT} – Recovery parameter related to TT.
[e] USE – Upper shelf energy.
[f] R^{USE} – Recovery parameter related to USE.
[g] A_F – Irradiation embrittlement coefficient.

hardness difference ΔHV between the hardness of the irradiated and unirradiated state is also given in Table 3 and covers a range 4.0–25.6. The highest values are observed for the VVER 1000 heats.

The effect of annealing is described by a recovery parameter R defined as the ratio of the residual property change after annealing to the change due to irradiation [16]. A value of 1 represents the fully recovered state.

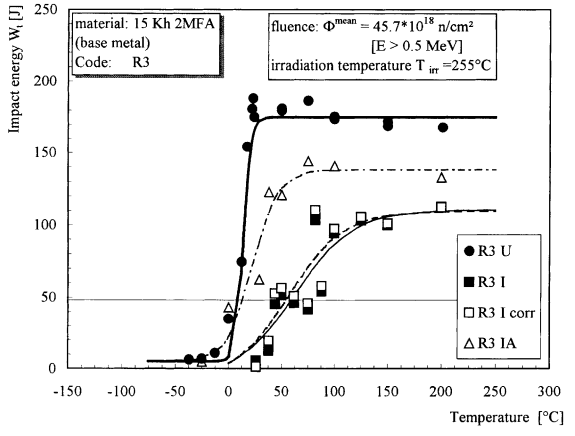

Fig. 1. Charpy V-notch impact energy–temperature curves of 15Kh2MFA (heat R3) steel in the unirradiated (U), irradiated (I) and annealed (IA) state.

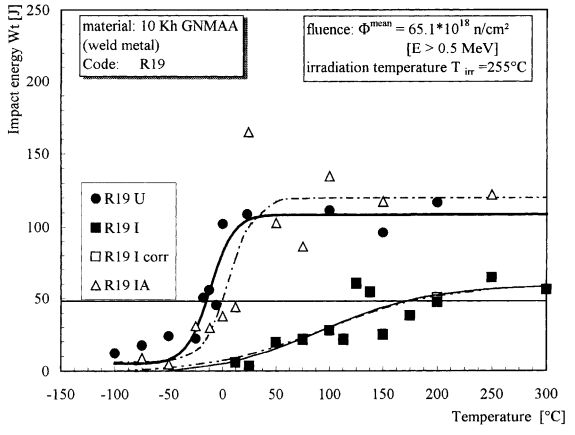

Fig. 2. Charpy V-notch impact energy–temperature curves of 10KhGNMAA weld metal (heat R19) in the unirradiated (U), irradiated (I) and annealed (IA) state.

Table 3
Vickers hardness HV10 (mean and standard deviation) of unirradiated (U), irradiated (I) and post-irradiation annealed (IA) specimens, hardness change ΔHV10 related to the unirradiated state, irradiation hardening coefficient A_F^{HV} and recovery parameter R^{HV}

Type	Code	State	Φ_{mean}[a] [10^{18} n/cm^2]	HV10	ΔHV10	A_F^{HV}	R^{HV}
15Kh2MFA	R1	U		236 ± 4			
		I	43.6	250 ± 5	14	4	
		IA		225 ± 3	−11		1.79
	R2	U		198 ± 3			
		I	80.7	269 ± 4	71	16.4	
		IA		210 ± 3	12		0.83
	R3	U		232 ± 4			
		I	45.7	281 ± 4	49	13.7	
		IA		246 ± 3	14		0.71
	D25	U		205 ± 4			
		I	127.6	258 ± 4	53	10.5	
		IA		240 ± 26	35		0.34
15Kh2NMFAA	R16	U		220 ± 6			
		I	46	305 ± 2	85	23.7	
		IA		240 ± 4	20		0.76
	R17	U		227 ± 5			
		I	72.7	292 ± 4	65	15.6	
		IA		260 ± 4	33		0.49
10KhGNMAA	R19	U		206 ± 7			
		I	65.1	309 ± 3	103	25.6	
		IA		239 ± 4	33		0.68

[a] Mean fluence [$E > 0.5$ MeV].

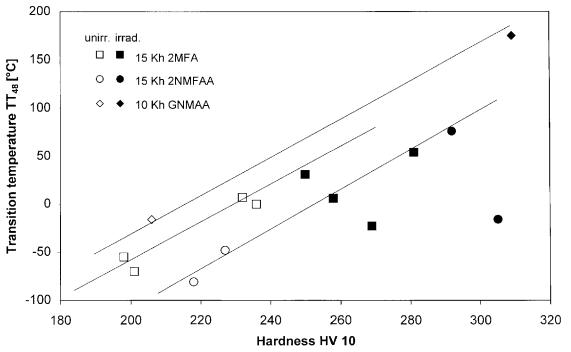

Fig. 3. Correlation between transition temperature TT_{48} related to the 48 J-energy-level and hardness HV10 for the materials tested in unirradiated and irradiated state.

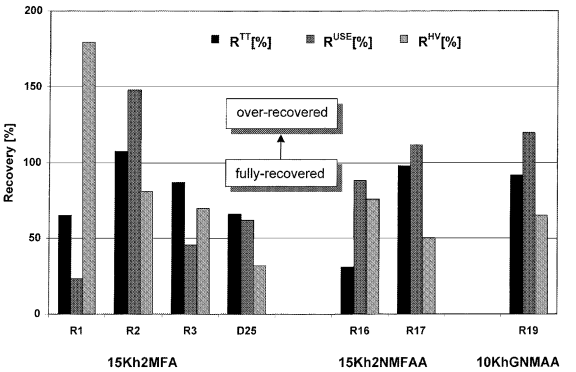

Fig. 4. Percent recovery of the transition temperature shift ΔTT_{48}, the upper shelf energy USE and the Vickers hardness HV10.

The recovery parameters R for the Charpy properties (TT, USE) and the hardness are given in Tables 2 and 3 and are depicted in the graph of Fig. 4. As a rule the Charpy parameters recover more fully than the hardness, but the ranking order for the different materials is not the same when indexed by the different parameters. A complete recovery of the Charpy parameters is observed for the heats R2, R17 and R19. Partly, they even exhibit 'over-recovery', above all regarding the USE values. Although similar behaviour was already reported [16,17] the differences between the different states are very low and the effect could be due to data scatter. It is to be noticed that the high irradiation effect of the VVER 1000 weld metal R19 is almost fully recovered.

4.2. SANS experiments

In all samples investigated irradiation produces an increase of SANS intensity in the range of the scattering vector Q of about 0.8–3 nm^{-1}. The increase distinguishes for the different heats. Annealing reduces the

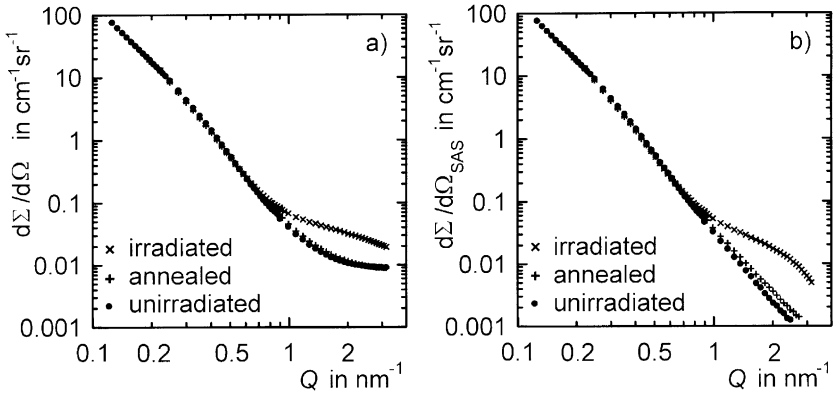

Fig. 5. Total macroscopic neutron scattering cross-section $d\Sigma/d\Omega$ for the 15Xh2NMFAA steel, heat R16, left: measured curve, right: corrected curve (subtraction of constant Laue contribution).

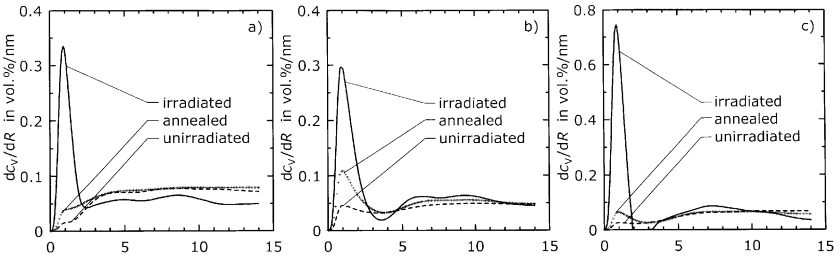

Fig. 6. Volume fraction-defect size distribution for (a) 15Xh2MFA (D25), (b) 15Xh2NMFAA (R17) and (c) 10KhGNMAA (R19) in unirradiated, irradiated and annealed states, respectively.

scattering intensity to a level that is comparable with the unirradiated state. Fig. 5 shows the scattering curve of heat 16 as an example. Furthermore, a constant Q-independent scattering contribution is observed. The contribution is caused by the incoherent scattering and the monotonic Laue scattering and must be excluded for the further analysis using the Porod approximation as described in [18]. It is mainly nuclear scattering and larger than the pure isotope effect. Irradiation enhances the constant scattering contribution in every case.

Typical size distribution curves determined by the Glatter procedure from the corrected scattering curve are depicted in Fig. 6. Irradiation has a clear effect only on the radius range from 0 to about 2 nm with the maximum near 1 nm.

Scattering particles with larger size are also existing. In this range there are hardly relevant differences between different material states. Therefore, the evaluation is focused on the range of $R \leqslant 2$ mm. These results are summarized in Table 4. A fraction of scattering features in the size range 0–2 nm already occurs in the unirradiated state. Whereas this fraction is small for the most heats and is probably rather a result of uncertainties of the indirect Fourier transformation method, this fraction is remarkable for the 15Kh2MFA heats R1 and R3. In these cases the irradiation-caused increase of the nanoscale defect fraction is low. For the other heats volume fractions of about 0.2–0.65% are produced by irradiation.

Table 4 contains the so-called A-ratio calculated from the ratio between the total and nuclear scattering cross-section. The A-ratio is not constant over the measured Q-range and is, therefore, only analysable if related to the size distribution [19]. The A-ratios given in Table 4 are calculated at the size distribution peak. The uncertainties are high for the unirradiated and the annealed specimens because the measuring effects are small. For the irradiated state the A-ratio is in the range 1.7–2.8. The highest values (2.5–2.8) are characteristic for the WWER 1000-type base and weld metal heats (R16, R17, R19).

5. Discussion

Irradiation phenomena are affected by a large number of environmental variables, mainly neutron fluence, material composition, metallurgical treatment and temperature. Apart from the irradiation temperature the irradiation programme comprises a wide variety of

Table 4
Results of the SANS experiments

Material	Code	State	Fluence (10^{18} n/cm^2)	R_{max} (nm)[a]	C_v (%)	ΔC_v (%)	A-ratio	$A_F^{MS}[10^{-3}]$[b]	R^{MSc}
15Kh2MFA	R1	U[d]			1.1	0.29		2.5	
		I[e]	43.6	1.0	0.32	0.03	2.2	0.69	
		IA[f]		–	–	–	–	–	n.m.[g]
	R2	U		>4	0.05		2.2		
		I	80.7	1.0	0.25	0.2	2.1	2.48	
		IA		–	–	–	–		n.m.
	R3	U		>4	0.23		2.2		
		I	45.7	1.0	0.28	0.05	2.4	1.09	
		IA		–	0.23	0.00	1.8		1.00
	D25	U		>4	0.04		2.1		
		I	127.6	1.0	0.35	0.31	1.7	2.43	
		IA		>4	0.08	0.04	2.6		0.87
15Kh2NMFAA	R16 U		>4	0.08		2.6			
		I	46	0.9	0.66	0.58	2.5	12.61	
		IA		1.0	0.12	0.04	2.5		0.93
	R17	U		>4	0.09		2.4		
		I	72.7	1.0	0.39	0.3	2.8	4.13	
		IA		1.0	0.17	0.08	2.4		0.73
10KhGNMAA	R19	U		>4	0.03		2.8		
		I	65.1	0.9	0.68	0.65	2.8	9.98	
		IA		1.0	0.08	0.05	2.6		0.93

[a] R_{max} – Radius at peak of size distribution.
[b] A_F^{MS} – Irradiation coefficient related to Eq. (3).
[c] R^{MS} – Recovery parameter related to ΔC_v.
[d] U – Unirradiated.
[e] I – Irradiated.
[f] IA – Post-irradiation annealed.
[g] n.m. – Not measured.

variables, e.g. fluences of 43–127.6 × 10^{18} n/cm^2, Ni content of 0.1–1.7%, Cu content of 0.04–0.13%, P content of 0.011–0.024%, and forged or welded microstructures, however, without varying them systematically. Under these circumstances the interpretation of the results is problematic.

Roughly, the variables can be subdivided in some groups through

- The Ni-poor Cr–Mo–V alloyed VVER 440-type RPV base metal with low Cu content (approx. 0.1%) and variation of the P content of 0.011–0.024% (R1 – R3, D 25).
- The Cr–Ni–Mo alloyed VVER 1000-type RPV base metal (R16, R17) with constant P content (approx. 0.12%) and different Ni and Cu contents.
- The Cr–Ni–Mo alloyed VVER 1000-type RPV weld metal with high Ni content and low Cu content.

These three groups show clearly different irradiation sensitivities. Fig. 7 compiles the fluence dependence of the transition temperature shift ΔTT_{48}. The lines describe the fluence dependence according to Eq. (1) using mean values for the irradiation coefficient A_F of the concerned material group. The irradiation sensitivity increases in the order of VVER 440-type RPV base metal, VVER 1000-type base metal and VVER 1000-type weld metal. A similar trend is observed using the hardness test results.

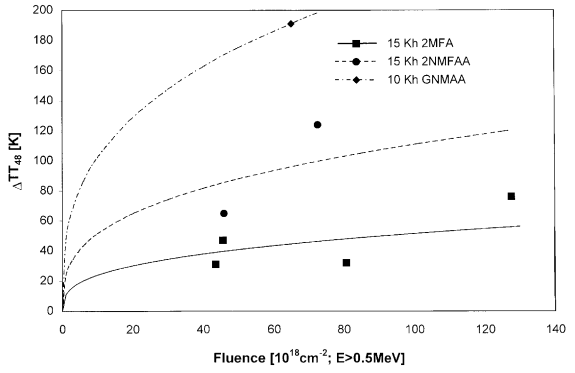

Fig. 7. Transition temperature shift ΔTT_{48} versus neutron fluence (line average curve according to Eq. (1)).

The sensitivity-to-irradiation embrittlement is estimated with the empirical formula [14]

$$A_F = 800(P + 0.07\ Cu), \quad (2)$$

where P and Cu are the contents of phosphorus and copper in mass percentage, respectively. The formula is strictly valid for VVER 440-type welds and the irradiation temperature 270°C but is also considered for VVER 440-type base metal [20] or VVER 1000-type base metal and weld [15,21].

Fig. 8 compares the experimental results of the irradiation embrittlement sensitivity A_F to the trend curve according to Eq. (2). Only the VVER 440-type base metals substantiate the trend curve, even in a conservative manner. The VVER 1000-type base and weld metal heats are not in accordance with the approach that the sensitivity against irradiation embrittlement is mainly a function of the contents of copper and phosphorus. Above all the high irradiation coefficient of the weld heat R19 cannot be explained on this basis.

The higher irradiation sensitivity of the VVER 1000-type RPV heats can be associated with the Ni content. Even more, also within these heats (and independent of the basic microstructure) the sensibility increases with increasing Ni content. In comparison to this, other parameters like Cu or P content or the microstructure (weld or base metal) seem to be less important. The detrimental effect of Ni on the irradiation embrittlement was described repeatedly for both VVER-type and Western RPV steels [22–25]. The Ni influence is especially significant for Ni contents >1% and the larger the Ni content the higher the fluence or the Cu content. Weld metal has no higher sensitivity in comparison to the base metal when the Ni content is the same [22]. Qualitatively, the transition temperature shift measured corresponds to these results.

SANS experiments provide a clear evidence of irradiation-induced microstructural features with a mean radius of approx. 1 nm. Similar features have been detected in Western RPV steels with both high and low Cu content and even due to electron radiation (e.g. [26–30]). Neither fluence nor material composition seems to have an effect on the size of these defects. Small differences of the radius R_{max} at maximum of the size distribution for the different heats are within the accuracy of the position of maxima, as determined by the indirect Fourier transformation method. The height of the maximum of the size distribution curve and so also the volume fraction of the defects increase with increasing fluence if the different steel types are considered separately. This is demonstrated in Fig. 9. For the 4 VVER 440-type RPV heats, the fluence dependence is approximately a simple linear function

$$\Delta C_v = A_F^{MS} \Phi, \tag{3}$$

where A_F^{MS} is a microstructure-related irradiation coefficient.

This coefficient hardly depends on the P content in correspondence to SANS experiments performed on a series of eight Fe-base model alloys with different P, Cu and Ni contents [31]. A strong effect has the Ni content. In each case the Ni-rich heats exhibit a higher volume fraction of nanoscale defects. However, the results does not show an unambiguous relation to the Ni content.

The volume fraction was calculated from the magnetic scattering cross-section under the assumption that the scattering features act as magnetic holes in a saturated ferromagnetic iron matrix. Thus, the magnetic scattering contrast is precisely known and the calculated volume fraction is independent of composition (but dependent on the particle shape). Composition and structure (number density) of the features control the nuclear scattering contrast. A high nuclear contrast yields a low A-ratio. The A-ratio is a little smaller for the VVER 440-type RPV heats than for the VVER 1000-type heats. With a maximum of 2.8 it is clearly smaller than expected for Cu-rich precipitates. As APFIM investigations [26,30,32,33] showed, in particular for RPV steels with low or medium Cu content more diffuse defects enriched with Ni, Mn, Si, P and Cu are formed. Ni seems to promote the process although the content of Ni

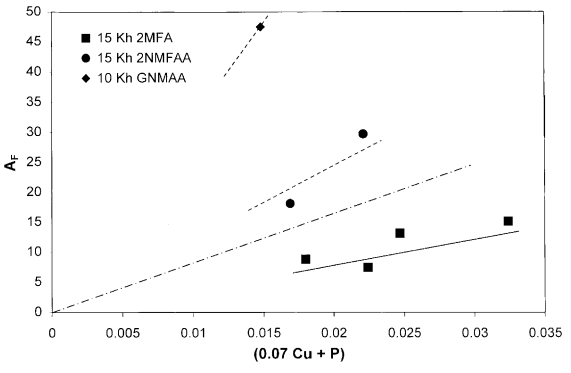

Fig. 8. Variation of experimental irradiation embrittlement coefficient A_F with a chemistry factor defined by Eq. (2).

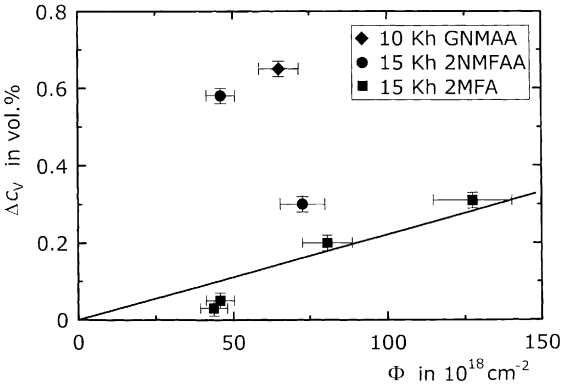

Fig. 9. Dependence of the volume fraction ΔC_v of the irradiation-induced microstructural defects on the neutron fluence Φ.

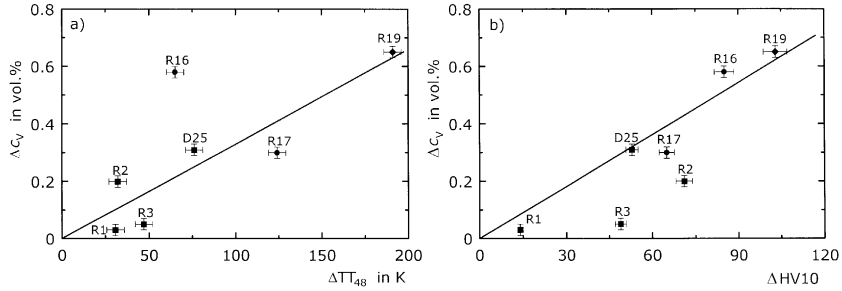

Fig. 10. Correlation between transition temperature shift ΔTT_{48}, (a) or change of hardness $\Delta HV10$, (b) and irradiation-induced volume fraction ΔC_v of nanoscale defects.

in the defects is relatively low. Depending on the composition and the fraction of vacancies, an A-ratio between 1.6 and 3.0 can be estimated. The differences of the scattering length between Fe and Ni are low but large between Fe and V [34]. This means that the Ni content in the nanoscale defects, as expected for the VVER 1000 heats, raises the A-ratio whereas V, as expected for the VVER 440 heats, lowers the A-ratio. The measured values are in accord with this model.

Fundamentally, the nanoscale fraction seems to be essential for the irradiation hardening and embrittlement of these steels. Fig. 10 shows the correlation between transition temperature shift and hardness change, respectively, and the irradiation-induced volume fraction of nanoscale defects. Although the scatter is considerable the trend is obvious: the higher the volume fraction the higher the embrittlement and the hardening. In the light of this correlation the unexpected high transition temperature shift of heat R19 is not extraordinary.

On the other hand, the appearance of outliers and the strong scatter prove that irradiation hardening and embrittlement cannot be estimated on the base of such simple parameter like the volume fraction of nanoscale defects. Obviously, there are additional factors of evidence, e.g. the hardening effectivity, which depends on the composition, structure and shape of the defects, the superposition of hardening effects caused by the preexisting fine precipitates like V- or Mo-carbides or by the matrix strengthening by solving foreign atoms, which is also changed due to the irradiation defect evolution.

Annealing yields a remarkable reduction of the irradiation effect. However, the recovery is different for the different parameters and heats. Related to the microstructure the nanoscale portion is nearly fully removed. This is apparently independent of fluence or composition and, hence, of initial microstructure. Since the shape of the size distribution curve is not changed, dissolution of the irradiation-induced defects is the most probable process. From the thermodynamic point of view this evolution is plausible for diffuse defects containing a mixture of vacancies, iron, manganese, silicium, nickel, phosphorus or copper atoms in different portions.

Despite the high degree of recovery of the microstructural parameter, the mechanical properties are only partly recovered in some cases (e.g. D25, R3, hardness of R17). Thus annealing does not only result in dissolution but in there are additional microstructural changes which are not resolved by SANS. Taking into consideration the test variables, the P content is a potential factor for the irreversibility of the irradiation effects in correspondence to the results described by Amaev et al. [35] for VVER 440 RPV steel.

6. Conclusion

Irradiation experiments at 255°C in a VVER-typical neutron field to mean neutron fluences between 43.7 and 127.6×10^{18} n/cm^2 [$E > 0.5$ MeV] yield information on the irradiation embrittlement and hardening sensitivity of VVER-type RPV steels.

The irradiation sensitivity depends on the type of steel and is higher for the Ni-rich VVER 1000 steel than for the Ni-poor VVER 440 steel. The radiation embrittlement of the VVER 440-type RPV steel heats is controlled by the Cu and P contents whereas the Ni content is decisive for VVER 1000-type RPV steel heats.

Both types of RPV steels exhibit microstructural features of a size distribution that is characterized by a narrow sharp peak at a radius of approx. 1 nm and a broader peak in the range of 5 mm up to >15 nm. Only the sharp first peak is changed by irradiation.

The irradiation-induced microstructural evolution can be described by the parameters volume fraction and size of fine-scale features, and the A-ratio. In comparison to the VVER 440-type steel heats, the VVER 1000-type RPV steel heats show a higher volume fraction and slightly higher values of the A-ratio whereas the size is equal. Different P contents do not change the microstructure analysed from SANS experiments.

The volume fraction of fine-scale features is an essential, but not the one factor that controls irradiation embrittlement and hardening.

By annealing (475°C/100 h) the fine-scale features are almost completely dissolved. In accord with this appearance, embrittlement and hardening are, at least partly, remedied.

Acknowledgements

The authors thank Miss M.H. Mathon from LLB Saclay, Mr P. Strunz from HMI Berlin and Mr C. Dewhurst from ILL Grenoble for supporting SANS measurements and for helpful discussions of the results. The SANS experiments at LLB were supported by the European Commission through the Access to Research Infrastructures action of the Improving Human Potential programme (contract no.: HPRI-CT-1999-00032). The work was sponsored by the Bundesministerium für Wirtschaft and Technologie (FRG) under contract GRS 1500919 and 15010120. The authors are grateful for the sponsorship.

References

[1] R. Ahlstrand, K. Törrönen, M. Valo, B. Bars, in: L.E. Steele (Ed.), Radiation Embrittlement of Nuclear Reactor Pressure Vessel Steels: An International Review, vol. 2, ASTM STP 909, PA, 1986, p. 55.
[2] H.-W. Viehrig, J. Böhmert, J. Dzugan, H. Richter, in: S.T. Rosinski, M.L. Grossbeck, T.R. Allen, A.S. Kumar, (Eds.), Effects of Radiation on Materials: 20th International Symposium, ASTM STP 1405, West Conshohocken, PA, accepted.
[3] H.-W. Viehrig, J. Böhmert, J. Dzugan, Bewertung des Bestrahlungsverhaltens russischer WWER-Reaktordruckbehälterstähle, 26. MPA-Seminar, Staatliche Materialprüfanstalt Stuttgart, 2000, p. 20.1.
[4] M. Brumovsky, Nucleon 3&4 (1993) 4.
[5] H.-U. Barz, B. Böhmer, J. Konheiser, I. Stephan, Ermittlung der Neutronendosis von bestrahlten WWER-Reaktordruckbehältermaterialien, Forschungszentrum Rossendorf e.V., Wissenschaftlich-technische Berichte, FZR-87, 1995.
[6] H.-W. Viehrig, H.-U. Barz, J. Böhmert, B. Böhmer, in: Proceedings of the IAEA Specialists Meeting, Vladimir, Russia, September 1997, IWG-LMNPP-97/2, Vienna, p. 230.
[7] U. Keiderling, A. Wiedenmann, Phys. B 213&214 (1995) 895.
[8] P. Lindner, R.P. May, P.A. Timmins, Phys. B 180&181 (1992) 967.
[9] Laboratoire Leon Brillouin: Equipments Experimentaux, Edition LLB, 1995, p. 69.
[10] P. Strunz, J. Saroun, U. Keiderling, A. Wiedemann, R. Przenioslo, J. Appl. Crystallogr. 33 (2000) 834.
[11] O. Glatter, J. Appl. Crystallogr. 13 (1980) 7.
[12] M. Grosse, J. Böhmert, R. Gilles, J. Nucl. Mater. 254 (1998) 143.
[13] M. Grosse, V. Denner, J. Böhmert, M.-H. Mathon, J. Nucl. Mater. 277 (2000) 280.
[14] R. Gerard, Survey of national regulatory requirements, AMES Report No. 4, Brussels, 1995, EUR 16305 EN.
[15] V. Prokovsky, Problems of assessement of pressure vessel VVER 1000 radiation lifetime, Workshop on VVER-RPV integrity assessment, methods and applications, February 2000, Cologne, Germany.
[16] M.A. Sokolov, R.K. Nanstad, S.K. Iskander, in: D.S. Gelles, R.K. Nanstad, A.S. Kumar, E.A. Little, (Eds.), Effect of Radiation on Material, vol. 17, ASTM STP 1270, American Society for Testing and Materials, PA, 1996, p. 690.
[17] S.K. Iskander, M.A. Sokolov, R.K. Nanstadt, in: R.K. Nanstad, M.L. Hamilton, F.A. Garner, A.S. Kumar, (Eds.), Effects of Radiation on Materials: 18th International Symposium, ASTM STP 1325, American Society for Testing and Materials, 1999, p. 403.
[18] M. Große, J. Böhmert, in: M.L. Hamilton, A.S. Kumar, S.T. Rosinski, M.L. Grossbeck, (Eds.), Effects of Radiation on Materials: 19th International Symposium, ASTM STP 1366, American Society for Testing and Materials, West Conshohocken, PA 2000, p. 323.
[19] M. Große, A. Gokhman, J. Böhmert, Nucl. Instrum. and Meth. B 160 (2000) 515.
[20] L.M. Davies, A comparison of western and eastern nuclear reactor pressure vessel steels, AMES Report No. 10, Oxford, 1997, EUR 17327 EN.
[21] O.M. Vishkarev, Yu.I. Zvezdiz, V.K. Shamardin, G.A. Tulyakov, in: L.E. Steele, (Ed.), Radiation Embrittlement of Nuclear Reactor Pressure Vessel Steels: An International Review, vol. 4, ASTM STP 1170, PA, 1993, p. 218.
[22] A.D. Amaev, D.Yu. Erak, A.M. Kryukov, in: Proceedings of the IAEA Specialists Meeting on Irradiation Embrittlement and Mitigation, Madrid, April 1999, p. 374.
[23] Pr.E. Grynik, L. Chyrko, V. Revka, O. Drogayev, Pr. J. Foct, R. Bertrand, C. Trollat, J.P. Massoud, in: Proceedings of the IAEA Specialists Meeting on Irradiation Embrittlement and Mitigation, Madrid, April 1999, p. 386.
[24] R. Langer, W. Backfisch, R. Bartsch, in: Proceedings of the IAEA Specialists Meeting on Irradiation Embrittlement and Mitigation, Madrid, April 1999, p. 308.
[25] J.R. Hawthorne, in: H.R. Brager, J.S. Perrin, (Eds.), Effects of Radiation on Materials, vol. 11, ASTM STP 782, American Society for Testing and Materials, PA, 1982, p. 375.
[26] J.T. Buswell, W.J. Phythian, R.J. McElroy, S. Dumbill, P.H.N. Ray, J. Mace, R.N. Sinclair, J. Nucl. Mater. 225 (1995) 196.
[27] M.H. Mathon, A. Barbu, F. Dunsteller, F. Maury, N. Lorenzelli, C.H. de Novion, J. Nucl. Mater. 245 (1997) 224.

[28] M.A. Sokolov, S. Spooner, G.R. Odette, B.D. Wirth, G.E. Lucas, in: R.K. Nanstadt, M.L. Hamilton, F.A. Garner, A.S. Kumar, (Eds.), Effects of Radiation on Materials: vol. 18, ASTM-STP 1325, American Society for Testing and Materials, West Conshohocken, PA, 1999, p. 333.
[29] B.D. Wirth, R. Odette, W.A. Ravinich, G.E. Lucas, S.E. Spooner, in: R.K. Nanstadt, M.L. Hamilton, F.A. Garner, A.S. Kumar, (Eds.), Radiation Effects on Materials, vol. 18, ASTM-STP 1325, American Society for Testing and Materials, West Conshohocken, PA, 1999, p. 102.
[30] P. Anger, P. Pareige, M. Akanatsu, J.-C. Van Duysen, J. Nucl. Mater. 211 (1994) 194.
[31] J. Böhmert, A. Ulbricht, A. Kruykov, Y. Nikolaev, D. Erak, in: S.T. Rosinski, M.L. Grossbeck, T.R. Allen, A.S. Kumar, (Eds.), Effects on the Radiation on Materials, 20th International Symposium, ASTM-STP 1405, American Society for Testing and Materials, West Conshohocken, PA, 2002.
[32] P. Pareige, M.K. Miller, Appl. Surf. Sci. 94/95 (1996) 370.
[33] G.R. Odette, G.E. Lucas, Radiat. Eff. Def. Solids 44 (1998) 189.
[34] G. Kostorz, S.W. Lovesey, in: G. Kostorz (Ed.), Neutron Scattering Treatise on Material Science and Technology, vol. 15, London, 1979.
[35] A.D. Amaev, A.M. Kryukov, V.I. Levit, P.A. Platonov, M.F. Rogov, M.A. Sokolov, in: Proceedings of the Plant Life Extension in Nuclear Facilities (PLEX), Zürich, 1993.